High-Pressure Vapor−Liquid Equilibrium for R-22 + Ethanol and R-22 + Ethanol + Water

Mohamed M. Elbaccouch, Michael B. Raymond, and J. Richard Elliott*

Department of Chemical Engineering, The University of Akron, Akron, Ohio 44325-3906

High-pressure vapor−liquid equilibrium (VLE) data for the systems CO_2 + methanol at 313.05 K, CO_2 + ethanol at 323.55, 325.15, and 333.35 K, R-22 (chlorodifluoromethane) + ethanol at 343.25, 361.45, and 382.45 K, and R-22 + ethanol + water at 351.55, 362.65, and 371.85 K are obtained using a circulation-type VLE apparatus. The apparatus is tested with measurements of the CO_2 + methanol and CO_2 + ethanol systems. The experimental data are correlated using the Peng−Robinson and Elliott−Suresh−Donohue equations of state.

Introduction

The use of supercritical fluid solvents (SCF's) and near-critical fluid solvents (NCF's) in chemical processes has been increasing steadily. SCF's have an advantage in that their solvating power can be enhanced or diminished by a slight change in pressure or temperature. Furthermore, they can solubilize materials at relatively low temperatures. There has been a particular interest in using CO_2 as a SCF because it is inexpensive, nontoxic, and not flammable and has low critical parameters (McHugh and Krukonis, 1986). The applications of SCF's have been investigated by many researchers. Tom et al. (1991) applied SCF's in the controlled release of drugs. Beckman and Smith (1990) used SCF's in microemulsion polymerization. Downey et al. (1994) used supercritical water oxidation to destroy hazardous military wastes. Beer and Peter (1985) used SCF's to extract lingnin from wood. Besides CO_2, a large number of SCF's could be selected for entrainment, but the ability to design such processes is limited by the availability of reliable data for characteristic solubilities.

One potential NCF entrainer is chlorodifluoromethane (R-22). R-22 is polar, and its properties can be compared with those of propane. The critical pressure of R-22 is 17% higher than that of propane, but the critical temperatures are nearly the same. The critical temperature and pressure of R-22 are 369.30 K and 4.97 MPa, respectively. One might speculate that the polarity of R-22 would make it more compatible with water and moderate the solution non-ideality between water and less polar substances such as ethanol. This manuscript addresses this issue by presenting data for R-22, ethanol, and water and comparing them with literature data for propane, ethanol, and water.

As a preliminary test, we tested our VLE measurement capability using systems for which literature data are available at similar conditions to those for the R-22 systems. The vapor−liquid equilibrium systems of CO_2 + methanol and CO_2 + ethanol were selected for comparison because they were well studied and the published data could be used to check the accuracy of our data. We found that our data agreed with those previous measurements.

* To whom correspondence should be addressed. Telephone: (330) 972-7253. Fax: (330) 972-5856. E-mail: dickelliott@uakron.edu.

Interest in systems containing CO_2 or propane with ethanol and water was originally motivated by an interest in recovering ethanol from water (Brignole et al., 1987; Horizoe et al., 1993). We would like to provide some indication of the viability of R-22 as an entrainer and relate this to propane. Also, the data presented in this work can be used to estimate the binary interaction parameters necessary to assess the prospects of recovering ethanol from water. We briefly address this issue in the discussion section.

In summary, we report the vapor−liquid equilibrium data of the binary systems CO_2 + methanol at 313.05 K, CO_2 + ethanol at 323.15, 325.15, and 333.35 K, and R-22 + ethanol at 343.25, 361.45, and 382.45 K. Also, we report the vapor−liquid equilibrium of the ternary system R-22 + ethanol + water at 351.55, 362.65, and 371.85 K, where the feed composition of ethanol to water is 95.6% to 4.4 wt % on a solvent-free basis (azeotropic composition). The experimental data were correlated using the Peng−Robinson equation of state (Peng and Robinson, 1976) and the Elliott−Suresh−Donohue equation of state (Elliott et al., 1990; Suresh and Elliott, 1992).

Experimental Section

Our experimental apparatus is a dynamic circulation continuous flow type where the vapor and the liquid are circulated inside the equilibrium cell thoroughly and continuously at a constant temperature until vapor−liquid equilibrium is achieved. The flow apparatus used in this work is represented schematically in Figure 1. It consists mainly of an equilibrium cell, two magnetic pumps, two sampling valves, two hand pumps, an oven, and a gas chromatograph.

Equilibrium Cell. The vapor−liquid equilibrium process is done in a Jerguson cell (Model 17-T-40) similar to the one used by Jennnings et al. (1991). The cell is made from type 316 stainless steel, has a volume of approximately 40 cm^3, and has a maximum working pressure of 34 MPa at 37 °C. The cell has rectangular glass windows on opposite sides, which provide visual confirmation that the experimental conditions are in the two-phase region.

10.1021/je990136g CCC: $19.00
Published on Web 02/09/2000

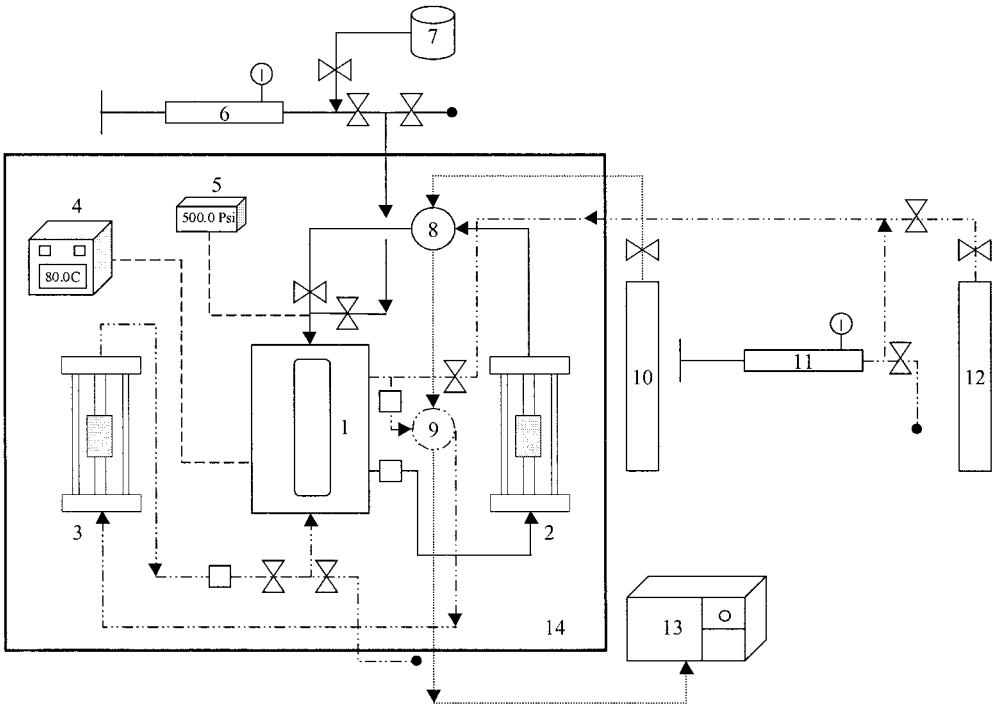

Figure 1. Schematic diagram of the VLE experimental apparatus: 1, equilibrium cell; 2, liquid magnetic circulation pump; 3, vapor magnetic circulation pump; 4, cell temperature indicator; 5, cell pressure indicator; 6, liquid feed high-pressure pump; 7, liquid reservoir; 8, liquid sampling valve; 9, vapor sampling valve; 10, helium cylinder; 11, gas feed high-pressure pump; 12, gas cylinder; 13, gas chromatograph; 14, constant-temperature air bath; —, liquid line; —••—, vapor line; •••, helium line; ●, vacum line; — — —, temperature or pressure probe; ⋈, valve; □, filter.

The cell's temperature is measured using an RTD probe manufactured by Omega Engineering (Model PR-17) connected to a temperature indicator manufactured by Omega Engineering (Model 4202A-PC2). The indicator has a 0.1 °C resolution and an accuracy of ±0.1 °C. The cell's pressure is measured using a Heise digital pressure indicator (Model 901-B) with a maximum working pressure of 41 MPa. The indicator has a resolution of 0.69 kPa and a rated accuracy of ±6.9 kPa. The temperature and the pressure indicators were calibrated by their manufacturers.

Magnetic Pumps. The circulation of the liquid and the vapor is achieved using Ruska magnetic circulation pumps (Model 2329-800). The pumps are made from type-316 stainless steel, have maximum flow rates of 100 $cm^3 \cdot min^{-1}$, and have a maximum working temperature and pressure of 177 °C and 124 MPa, respectively. A drive motor (Model NSH-11D3) and a motor speed controller are used to control the flow rates of the magnetic pumps.

Sampling Valves. The liquid sampling is done using a four-port Valco sampling valve (Model DCI4WTY0.5) which has an internal sample loop of 0.5 μL. The vapor sampling is done using a ten-port Valco sampling valve (Model 6C10WEY) which has a sample loop of 31.0 μL. The maximum operating temperature and pressure of the liquid and vapor sampling valves are 300 °C, 10 MPa and 125 °C, 27 MPa, respectively. The vapor sampling loop was calibrated to one decimal point by Valco.

Hand Pumps. The liquid is fed into the cell using a 30 cm^3 capacity liquid hand pump (Model 62-6-10). The gas is fed into the cell using a 60 cm^3 capacity liquid hand pump (Model 87-6-5) and cooling with dry ice. Both pumps were manufactured by High Pressure Equipment Company. The maximum working pressures of the liquid and gas feed pumps are 69 and 35 MPa, respectively.

Oven. The equilibrium cell, the magnetic pumps, and the sampling valves are placed inside a constant-temperature air bath (Model MH-5) manufactured by Forma Scientific. A new heating system was installed for the oven, which consists of a temperature controller (Model 4202A-PC2), and an external relay (Model MC1-2-30-120). Both items were manufactured by Omega Engineering.

Table 1. GC Conditions of System Studied

system	column	flow rate/ $cm^3 \cdot min^{-1}$	t_{oven}/ °C
methanol + CO_2	8 ft Pora Pak Q	64.86	135
ethanol + CO_2	12 ft Pora Pak Q	38.18	190
R-22 + ethanol	8 ft Pora Pak Q	87.69	125
R-22 + ethanol + water	10 ft Hayesep-D	44.74	130

Gas Chromatograph (GC). Data are analyzed using a Hewlett-Packard gas chromatograph (Model 5890) and an integrator (Model 3390 A). The GC is used to measure the relative amounts of the components in the two phases. A thermal conductivity detector (TCD) is used for all of the systems studied. The injection temperature was set to 200 °C, and the detector temperature of the GC was set to 250 °C for all of the systems studied. Helium is used as the carrier gas and as the reference gas for the detector. The flow rate of the carrier gas is measured using a digital flow meter (Model 520) manufactured by Humonics Incorporation. The flow rate of the carrier gas is measured while the reference gas is off. Table 1 contains a list of the packed columns, the flow rates of the carrier gas, and the oven's temperature for each system studied.

Procedures. The system was flashed and vacuumed several times with the gas of interest to remove any traces of air. Gas then was fed into the system using a liquid hand pump covered with dry ice. Once the liquid was fed into the system, the magnetic pumps were turned on and the oven temperature was set to the desired temperature. The circulation rates of the vapor and the liquid magnetic pumps had no effect on the equilibrium composition as long as liquid drops and vapor bubbles could be seen circulating

inside the cell through the glass window. Although Yoon et al. (1993) reported that the circulation rate affected the compositions of their system, our observation was that the circulation rates of the pumps affected only the equilibration time.

The vapor sampling valve and the line connecting the cell to the vapor sampling valve were set to a temperature 15 to 20 °C above the cell's temperature to prevent any condensation of vapor. The carrier gas line (helium) was heated to about 160 °C to ensure that no condensation occurred in the tubing while sampling was taking place. Equilibrium was reached when the temperature and the pressure of the system did not change over a period of at least 1 h. Three to four hours was typically the time required to reach equilibrium. Equilibrium condition was maintained by using small sampling loops. Also, the handles of the sampling valves were located outside the air bath, so that sampling occurred without opening the oven and disturbing the equilibrium temperature.

Vapor sampling was done first (while both magnetic pumps were on); then the vapor magnetic pump was turned off for about 15 min before the liquid samples were taken. However, we noticed that sampling the vapor phase before or after sampling the liquid phase had no effect on the equilibrium compositions. Moreover, it made no difference if sampling the liquid was done while the vapor sampling pump was on or off. When equilibrium was reached, liquid and vapor samples were taken by circulating through the sampling valve for at least 1 min for liquid samples and 30 s for vapor samples.

Five samples of each phase were taken for analysis by the GC, and the reported compositions were the result of averaging those samples together. The standard deviation of the liquid-phase compositions was within ±0.001 mole fraction, and that of the vapor-phase compositions was within ±0.0001. The maximum pressure drop in the system after withdrawing five samples from each phase was 0.69 kPa.

GC Calibrations. The GC was calibrated by plotting the number of moles of the component versus peak area. Calibrations for components that are vapors at ambient conditions were done by pressurizing the cell with a pure gas and reporting peak areas at a constant temperature and pressures ranging from 1.15 bar to a sufficient pressure to encompass all areas to be observed during the measurement phase (Yoon et al., 1993). The mass of the vapor corresponding to the analyzed peak area was calculated from the precisely known volume of the vapor sampling loop (31.0 μL) and the known CO_2 and R-22 densities obtained from Vargaftik (1975) and Dupont (1964), respectively.

Calibrations for liquids at ambient conditions were done by injecting known volumes of liquid into the GC via a Chaney adapter and a 7101-N Hamilton 1 μL syringe. The larger the volume injected into the GC by the syringe, the smaller the standard deviation of the GC areas. Thus, instead of injecting 0.3 μL of pure methanol, for instance, into the GC, we injected a larger volume of methanol diluted with 2-propanol. The pure methanol injection method and the diluted methanol injection method provided the same GC areas, but the latter gave a better area reproducibility than the former. The mass of the component injected was then calculated from the known density of the component and the volume injected.

Every composition point in the calibrated curves was a result of averaging five samples together. The calibration curves covered the entire range of the areas encountered in the experiments. Each calibration curve was divided into a high range and a low range. The data were fit with quadratic equations for which the *y*-intercepts were set equal to zero.

Table 2. Vapor−Liquid Equilibria of the CO_2 (1) + Methanol (2) System

T/K	*P*/MPa	*x*(1)	*y*(1)
313.05	1.139	0.0680	0.9730
313.05	1.808	0.1098	0.9815
312.85	2.822	0.1740	0.9864
313.25	3.577	0.2219	0.9877
313.25	4.274	0.2676	0.9882
312.95	4.641	0.2965	0.9885
313.05	5.371	0.3494	0.9882
313.15	6.121	0.4135	0.9874
313.15	6.845	0.4890	0.9858
313.05	7.220	0.5450	0.9840
312.95	7.534	0.5994	0.9819

It was necessary to do the vapor calibrations while the vapor magnetic pump was on. We found that the GC areas of the vapor calibration curves obtained while the vapor magnetic pump was on were significantly different from those obtained while the vapor magnetic pump was off. On the other hand, having the liquid magnetic pump on or off would not affect the outcome of the GC areas of the vapor calibration curves.

The average deviations in each of the vapor and liquid calibrations were within 0.2% and 3%, respectively. These percentages were based on the error between the correlated number of moles and the experimental number of moles, obtained using the vapor sampling device for vapors and the hand syringe for liquids. The deviations in our calibrations were similar to those reported by Suzuki and Sue (1990), who reported 1% and 3% error in the vapor and liquid calibrations, respectively, and Leu and Robinson (1992), who reported 2% error in the liquid calibration.

Chemicals. Helium of minimum purity 99.99% and carbon dioxide of 99.99% purity were obtained from Praxair Corporation. A 99.9% pure R-22 was obtained from Allied Signal. The purity of the gases was verified with the gas chromatograph. Methanol (99.9%) was obtained from Aldrich Chemical Co. Absolute ethanol (200 proof) was obtained from Quantum Chemical Corporation. Distilled water was obtained from the chemistry department at the University of Akron. All chemicals were used without any further purification.

Results and Discussion

Vapor−liquid equilibrium data for CO_2 + methanol at 313.05 K are presented in Table 2. Figure 2 shows a comparison between our results and the results reported by Ohgaki and Katayama (1976) at 313.15 K, Yoon et al. (1993) at 313.2 K, and Suzuki and Sue (1990) at 313.4 K. Figure 3 is a plot of the log *K* values of CO_2 and methanol versus pressure of our data and the literature data. Both figures show that our data agree very well with literature data.

Vapor−liquid equilibrium data for the system CO_2 + ethanol at 323.55, 325.15, and 333.35 K are presented in Table 3. A significant inconsistency exists in the literature between the VLE data of the CO_2 + ethanol system at 333.35 K reported by Suzuki and Sue (1990) and those reported by Nagahama et al. (1988) at 333.27 K. We reproduced that system at that particular temperature in order to check which set of data was more reliable. Figures 4 and 5 are plots of the pressure versus composition and the log *K* value versus pressure, respectively, of our results

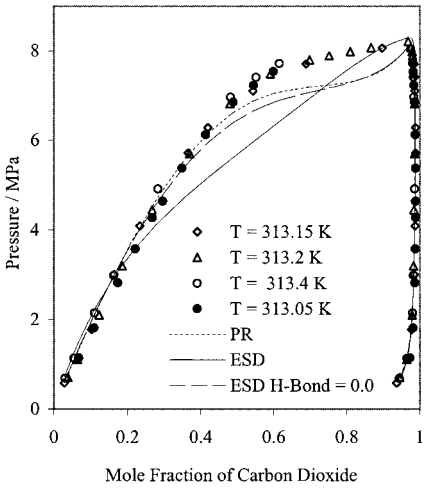

Figure 2. Experimental and literature VLE values of the carbon dioxide (1) + methanol (2) system: ◇, Ohgaki and Katayama (1976); △, Yoon et al. (1993); ○, Suzuki and Sue (1990); ●, this work.

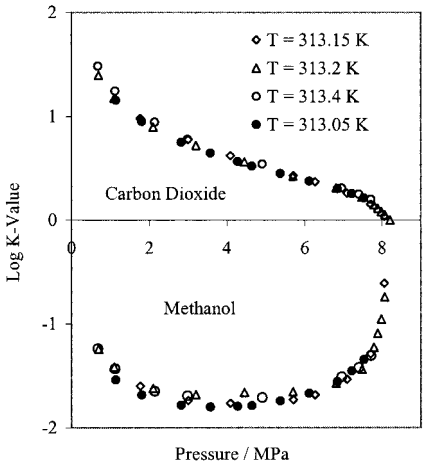

Figure 3. Log *K* value versus pressure for the carbon dioxide (1) + methanol (2) system: ◇, Ohgaki and Katayama (1976); △, Yoon et al. (1993); ○, Suzuki and Sue (1990); ●, this work.

and the results of Suzuki and Sue (1990) and Nagahama (1988). The figures show that our data agree very well with the values of Suzuki and deviate from the results of Nagahama.

Figure 6 shows that our pressure versus composition measurements of the system CO_2 + ethanol at 323.55 and 325.15 K agree very well with the values of Feng et al. (1988) at 323.4 K and the values of Jennings et al. (1991) at 325.16 K. However, a plot of the log *K* values versus the pressure shows that there is inconsistency in the vapor-phase measurements reported by Feng (Figure 7). Table 4 and Figure 8 present VLE data for the system R-22 + ethanol at 343.25, 361.45, and 382.45 K. The results of Xu et al. (1991) at 343.3 and 361.7 K agree well with our data. However, the data of Xu et al. at 382.7 K are inconsistent with our data at R-22 liquid mole fraction between 0.6 and 0.8. Our measurements indicate a slightly lower solubility of R-22 in the liquid.

With these measurements as background, we would like to comment briefly on the issue of sampling technique. The sampling method of Suzuki and Sue (1990) is similar to that proposed by Tsang and Street (1981) and Radosz (1986), who evaporated and homogenized the condensed-phase samples prior to on-line analysis. In preliminary studies of these systems, we implemented a homogenizer,

Table 3. Vapor−Liquid Equilibria of the CO_2 (1) + Ethanol (2) System

T/K	*P*/MPa	*x*(1)	*y*(1)
323.55	4.295	0.2124	0.9873
323.55	4.788	0.2440	0.9874
323.45	5.418	0.2829	0.9874
323.45	5.861	0.3125	0.9871
325.15	6.923	0.3831	0.9850
325.05	7.726	0.4568	0.9827
325.25	8.383	0.5303	0.9797
325.25	9.055	0.6433	0.9726
333.15	0.729	0.0285	0.9345
333.25	1.466	0.0589	0.9650
333.35	2.503	0.1056	0.9756
333.35	3.671	0.1565	0.9802
333.45	4.336	0.1880	0.9811
333.45	4.739	0.2082	0.9811
333.35	5.927	0.2721	0.9819
333.45	6.541	0.3074	0.9809
333.45	7.844	0.3962	0.9786
333.45	8.288	0.4369	0.9767
333.35	8.991	0.4931	0.9728
333.45	9.465	0.5222	0.9680
333.45	4.572	0.2006	0.9814
333.45	5.351	0.2413	0.9814

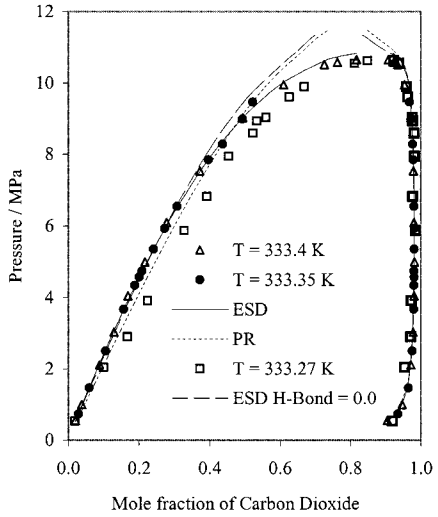

Figure 4. Experimental and literature VLE values of the carbon dioxide (1) + ethanol (2) system: △, Suzuki and Sue (1990); □, Nagahama et al. (1988); ●, this work.

but we found no significant change in the measured properties. Therefore, in this work we followed the method adapted by Ohgaki and Katayama (1976), Feng et al. (1988), Jennings et al. (1991), and Yoon et al. (1993), where a homogenizer was not used while sampling. The good agreement between our results and the results reported by Suzuki and Sue for the CO_2 + methanol and CO_2 + ethanol systems shows that a homogenizer is not necessary to obtain accurate VLE results. From our experience, the key consideration is to perform the vapor calibration directly from the sampling system of the apparatus itself within the range of the experimentally observed GC area.

New data for the ternary system R-22 + ethanol + water at 351.55, 362.65, and 371.85 K are reported in Table 5, and their isothermal VLE data are plotted in Figure 9. The relative volatilities of water and ethanol with respect to R-22 are reported in Table 5. A direct comparison between these data and the data for propane of Horizoe et al. (1993) is possible for the isotherm at 363 K, as shown in Figure 10a. Along this isotherm, the *K* value for R-22 is always lower than the *K* value for propane, despite the observation that the vapor pressure of R-22 is higher than that of

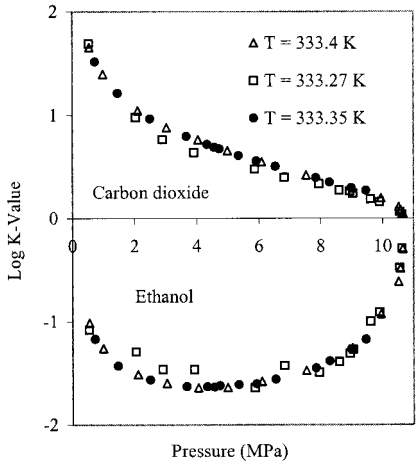

Figure 5. Log *K* value versus pressure for the carbon dioxide (1) + ethanol (2) system: △, Suzuki and Sue (1990); □, Nagahama et al. (1988); ●, this work.

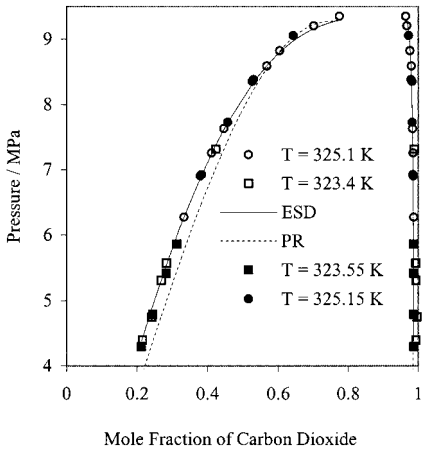

Figure 6. Experimental and literature VLE values of the carbon dioxide (1) + ethanol (2) system: ○, Jennings et al. (1991); □, Feng et al. (1988); ● and ■, this work.

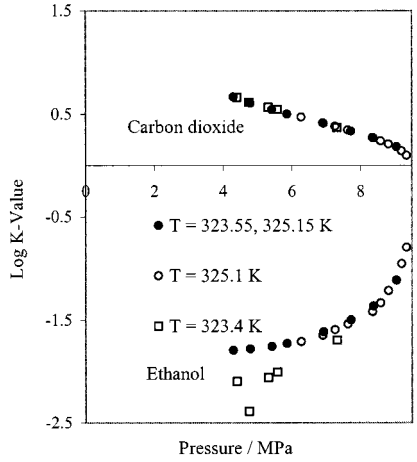

Figure 7. Log *K* value versus pressure for the carbon dioxide (1) + ethanol (2) system: ○, Jennings et al. (1991); □, Feng et al. (1988); ● and ■, this work.

propane. This is a reflection of the more ideal mixing between R-22 and water induced by the polar nature of R-22. Hence, the conjecture that R-22 should be more compatible than propane with water is supported. Regarding the relative volatility, the relative volatility of water is more favorable for R-22 than for propane for all pressures in this study, as shown in Figure 10b. Furthermore, the separation between the water volatility and the ethanol

Table 4. Vapor−Liquid Equilibria of the R-22 (1) + Ethanol (2) System

T/K	*P*/MPa	*x*(1)	*y*(1)
343.25	0.545	0.1226	0.8698
343.25	0.896	0.2104	0.9196
343.25	1.181	0.2847	0.9374
343.25	1.667	0.4320	0.9540
343.25	2.114	0.6242	0.9648
343.25	2.368	0.7304	0.9699
343.25	2.461	0.7830	0.9725
343.25	2.559	0.8324	0.9753
343.25	2.740	0.9039	0.9823
361.45	0.627	0.0928	0.7677
361.45	1.387	0.2418	0.8884
361.45	1.995	0.3694	0.9182
361.45	2.562	0.5174	0.9342
361.45	2.896	0.6209	0.9414
361.45	3.399	0.7875	0.9536
361.45	3.659	0.8579	0.9623
382.35	0.548	0.0330	0.4338
382.65	1.469	0.1659	0.7746
382.35	2.293	0.2933	0.8446
382.45	2.698	0.3595	0.8633
382.45	3.003	0.4126	0.8735
382.35	3.485	0.5050	0.8864
382.75	3.972	0.5930	0.8933
382.85	4.317	0.6663	0.8995
382.65	4.658	0.7432	0.9064
382.35	4.887	0.7915	0.9104

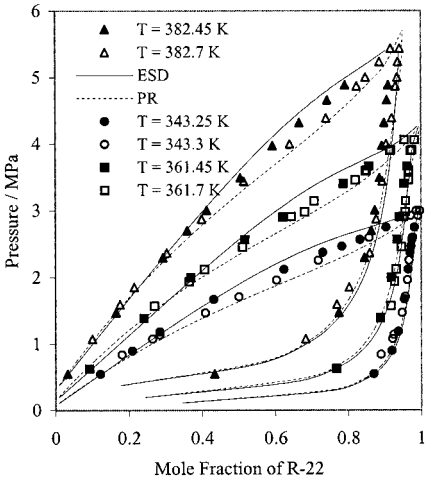

Figure 8. Experimental and literature VLE values of the R-22 (1) + ethanol (2) system: ○, □, and △, Xu et al. (1991); ●, ■, and ▲, this work.

volatility is more favorable with R-22. Once again, R-22 has altered the solution nonideality, this time by solubilizing more solvent into the liquid phase and volatilizing more water out of the liquid phase. What is less clear is the behavior of the relative volatility at pressures above those studied here. The data for propane show a sharp rise in the relative volatility of water. Note, however, that the cricondenbar at this temperature is near 4 MPa, so operation of a solvent recovery column at that condition would not be feasible. With respect to the solvent extraction column, Horizoe et al. (1993) suggest operating at pressures near 9.9 MPa for dehydration using propane. Such a high pressure would be above the cricondenbar for either NCF, even at 372 K, the highest temperature of the present study. Therefore, the extraction using propane relies on the formation of LLE at very high pressures and the NCF concentration. The conditions of our study do not encompass the pressure range where formation of such a second liquid phase (or dense SCF phase) might be observed. Considering the more ideal nature of the mixtures with

Table 5. Vapor−Liquid Equilibria of the R-22 (1) + Ethanol (2) + Water (3) System

T/K	*P*/MPa	*x*(1)	*x*(2)	*x*(3)	*y*(1)	*y*(2)	*y*(3)	α_{21}[a]	α_{31}
351.55	0.662	0.1267	0.8487	0.0246	0.8837	0.1128	0.0035	0.019	0.020
351.55	1.407	0.3043	0.6758	0.0199	0.9411	0.0570	0.0019	0.027	0.031
351.45	1.577	0.3493	0.6326	0.0181	0.9457	0.0525	0.0018	0.031	0.037
351.45	1.843	0.4269	0.5572	0.0159	0.9520	0.0463	0.0017	0.037	0.048
351.65	1.887	0.4375	0.5462	0.0163	0.9528	0.0454	0.0018	0.038	0.051
351.45	1.995	0.4709	0.5144	0.0147	0.9545	0.0438	0.0017	0.042	0.057
351.45	2.197	0.5402	0.4470	0.0128	0.9578	0.0407	0.0015	0.051	0.066
351.55	2.304	0.5811	0.4067	0.0122	0.9594	0.0389	0.0017	0.058	0.084
351.45	2.476	0.6474	0.3420	0.0106	0.9615	0.0368	0.0017	0.072	0.108
351.55	2.977	0.8512	0.1444	0.0044	0.9701	0.0282	0.0017	0.171	0.339
362.65	0.876	0.1386	0.8369	0.0245	0.8581	0.1375	0.0044	0.027	0.029
362.65	1.278	0.2183	0.7594	0.0223	0.8984	0.0982	0.0034	0.031	0.037
362.65	1.511	0.2677	0.7111	0.0212	0.9122	0.0849	0.0029	0.035	0.040
362.75	1.880	0.3507	0.6306	0.0187	0.9248	0.0725	0.0027	0.044	0.055
362.75	1.992	0.3762	0.6058	0.0180	0.9280	0.0694	0.0026	0.046	0.059
362.75	2.308	0.4557	0.5299	0.0144	0.9352	0.0625	0.0023	0.057	0.078
362.65	2.652	0.5535	0.4336	0.0129	0.9407	0.0569	0.0024	0.077	0.110
362.65	2.983	0.6572	0.3333	0.0095	0.9453	0.0525	0.0022	0.110	0.161
362.75	3.107	0.6980	0.2938	0.0082	0.9495	0.0483	0.0022	0.121	0.197
362.55	3.271	0.7527	0.2407	0.0066	0.9496	0.0482	0.0022	0.159	0.264
362.55	3.375	0.7850	0.2091	0.0059	0.9514	0.0464	0.0022	0.183	0.308
362.65	3.546	0.8336	0.1616	0.0048	0.9543	0.0435	0.0022	0.235	0.400
371.85	0.668	0.0759	0.8984	0.0257	0.7411	0.2509	0.0080	0.029	0.032
371.85	1.319	0.1900	0.7871	0.0229	0.8603	0.1351	0.0046	0.038	0.044
371.85	1.670	0.2548	0.7238	0.0214	0.8842	0.1120	0.0038	0.045	0.051
371.75	1.921	0.3022	0.6776	0.0202	0.8952	0.1014	0.0034	0.051	0.057
371.75	2.099	0.3368	0.6440	0.0192	0.9017	0.0949	0.0034	0.055	0.066
371.75	2.264	0.3712	0.6105	0.0183	0.9057	0.0910	0.0033	0.061	0.074
371.75	2.539	0.4313	0.5523	0.0164	0.9131	0.0837	0.0032	0.072	0.092
371.75	2.641	0.4564	0.5280	0.0156	0.9146	0.0823	0.0031	0.078	0.099
371.75	2.884	0.5122	0.4737	0.0141	0.9179	0.0790	0.0031	0.093	0.123
371.95	3.065	0.5581	0.4292	0.0127	0.9198	0.0771	0.0031	0.109	0.148
371.85	3.738	0.7368	0.2556	0.0076	0.9281	0.0688	0.0031	0.214	0.324

[a] α_{21} ≡ relative volatility of ethanol with respect to R-22.

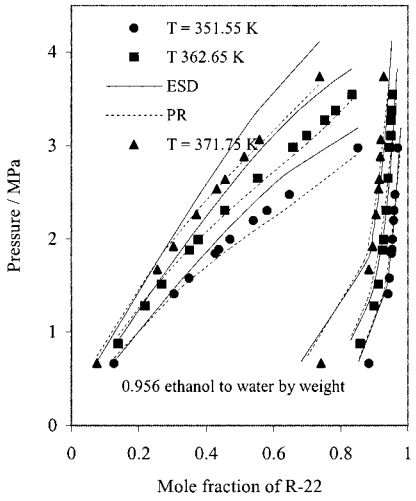

Figure 9. *P*−*T*−*x* diagram of the R-22 (1) + ethanol (2) + water (3) system: ●, ■, and ▲, this work.

R-22, it is entirely possible that no such phase will form. Hence, a definitive assessment of R-22 as an NCF in the kind of process envisioned by Brignole et al. (1987) must await LLE measurements at pressures near 10 MPa.

The experimental data were correlated using the Peng−Robinson equation of state (PR-EOS) (Peng and Robinson, 1976) and the Elliott−Suresh−Donohue equation of state (ESD-EOS) (Elliott et al., 1990; Suresh and Elliott, 1992). The ESD-EOS is a semiempirical model for the representation of thermodynamic properties for nonspherical and associating mixtures. It accounts for self-association and cross-association for systems with multiple associating species. In the present work, the hydrogen-bonding analysis was fully implemented in the sense that cross-association was included between solvate species such as CO_2 and ethanol. Table 6 contains the binary interaction parameters (k_{ij}) and the percentage error in the bubble point pressure (PAAD) for the ESD-EOS and the PR-EOS.

The interaction parameters of the R-22 + water system and the ethanol + water system, which were used to model the ternary system, were obtained by fitting the experimental data reported by Bennett (1966) and Gmehling et al. (1981), respectively. Since the experimental temperatures of the R-22 + ethanol + water system are different from those of the R-22 + ethanol system, the R-22 + water system, and the ethanol + water system, a temperature-dependent binary interaction parameter was used for the VLE calculation of the ternary system. This function is given by $k_{ij} = k_{ij}^{\circ} + k_{ij}^{T}/T$. T is the temperature in Kelvin, k_{ij}° is the temperature independent interaction parameter, and k_{ij}^{T} gives the temperature dependence of interaction parameter. Values of k_{ij}°, k_{ij}^{T}, and PAAD for the ternary system are listed in Table 7.

In the case of the ethanol + CO_2 system, the ESD-EOS, with a cross-association of hydrogen bonding equal to 17.17 kJ·mol^{-1}, fits the experimental data better than the PR-EOS does. Since the data reported by Nagahama et al. (1988) do not agree with our data and the data reported by Suzuki and Sue (1990), Nagahama's data were not used in regressing the ESD-EOS and the PR-EOS models.

In the case of the methanol + CO_2 system, the PR-EOS fits the experimental data better than the ESD-EOS, as shown in Figure 2. Figures 2 and 4 show that the results from the ESD-EOS coincide with those of the PR-EOS if the self-association of methanol and ethanol is ignored. Thus, the complexity of the carbon dioxide + methanol system must be related to details of the treatment of the hydrogen bonding, coupled with the mixing rules on the

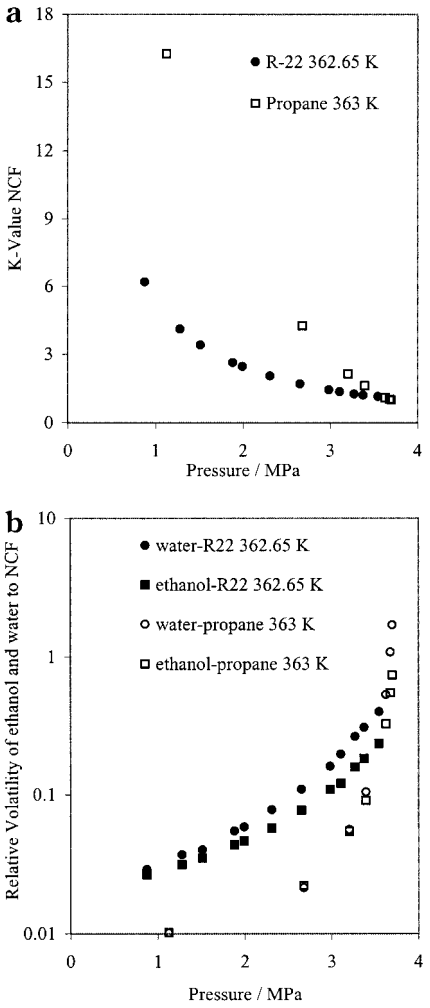

Figure 10. (a) *K*-value of R-22 in the R-22 + ethanol + water system at 362.65 K and of propane in the propane + ethanol + water system at 363 K in 95.6% ethanol by weight on a NCF-free basis: □, Horizoe et al. (1993); ●, this work. (b) Relative volatility of ethanol and water with respect to R-22 at 362.65 K and propane at 363 K in 95.6% ethanol by weight on a NCF-free basis: ○ and □, Horizoe et al. (1993); ● and ■, this work.

Table 6. k_{ij} Binary Interactions

system	temp/K	ESD K_{ij}	PR K_{ij}	%PAAD[a] ESD	%PAAD PR
methanol + CO_2	313.05	0.06626	0.0625	13.7	6.6
methanol + CO_2; H-Bond = 0.0	313.05	0.009622		7.8	
ethanol + CO_2	325.15	0.09062	0.0895	0.8	3.8
ethanol + CO_2	333.35	0.08597	0.095	1.0	7.0
ethanol + CO_2; H-Bond = 0.0	333.35	0.03695		3.4	
ethanol + R-22	343.35	−0.03682	−0.0047	4.9	5.7
ethanol + R-22	361.45	−0.04207	0.0134	4.4	3.9
ethanol + R-22	382.45	−0.03753	0.0195	4.9	3.9

[a] %PAAD ≡ percentage pressure average absolute deviation.

physical interactions. Huang and Radosz (1991) were able to correlate this system by developing a specialized mixing rule. We had hoped that some combination of cross-association and self-association might explain these trends in a less empirical manner, but the switch from low solubility to high solubility was always apparent when self-association of methanol was included. These considerations prompt a study of generalized mixing rules that will be undertaken in the future.

Table 7. k_{ij} Binary Interactions for the R-22 + Ethanol + Water System

system	k_{ij}° ESD	k_{ij}^{T} ESD	k_{ij}° PR	k_{ij}^{T} PR	%PAAD[a] ESD	%PAAD PR
R-22 + ethanol	−0.0593	7.9998	0.1913	−65.9291	3	5.1
R-22 + water	0.2438	−54.328	0.1597	−117.428	7.1	5.2
ethanol + water	0.1496	−41.1567	−0.0038	−30.1124	1.8	4.3

[a] %PAAD ≡ percentage pressure average absolute deviation.

Literature Cited

Beckman, E.; Smith, R. Microemulsion Polymerization Within Near- and Supercritical Continuous Phases: Effect of Microemulsion Structure on Reaction Characteristics. *J. Supercrit. Fluids*, **1990**, *3*, 205−213.

Beer, R.; Peter, S. High-Pressure Extraction of Lignin from Wood. In *Supercritical Fluid Technology, Processing Technology Proceedings, 3*; Penninger, J., Radosz, M., McHugh, M., Krukonis, V., Eds.; Elsevier: New York, 1985; pp 385−396.

Bennett, E. Technology Bulletin B-43; E. I. Du Pont de Nemours & Co., Freon Product Division, April 1966.

Brignole, E.; Anderson, P.; Fredenslund, A. Supercritical Fluid Extraction of Alcohol From Water. *Ind. Eng. Chem. Res.* **1987**, *26*, 254−261.

Downey, K.; Snow, R.; Hazlebeck, D.; Roberts, A. *Corrosion and Chemical Agent Destruction: Research on Supercritical Water Oxidation of Hazardous Military Wastes*; ACS Symposium Series 608; American Chemical Society: Washington, DC, 1995; pp 313−326.

Du Pont. *Thermodynamic Properties of Freon-22 Refrigerant*; E. I. Du Pont de Nemours & Co., Freon Products Division: 1964.

Elliott, J.; Suresh, S.; Donohue, M. A Simple Equation of State for Nonspherical and Associating Molecules. *Ind. Eng. Chem. Res.* **1990**, *29*, 1476−1485.

Feng, Y.; Du, X.; Li, C.; Hou, Y. *An Apparatus for Determining High-Pressure Fluid Phase Equilibria and Its Applications to Supercritical Carbon Dioxide Mixtures.* Proceedings of the International Symposium on Supercritical Fluids, October 17−19, Nice, France; Societe Francaise de Chimie: Paris, 1988; Vol. 1, pp 75−84.

Gmehling, J.; Onken, U.; Arlt, W. *Vapor-Liquid Equilibrium Data Collection*; Chemistry Data Series; Dechema: Frankfurt, 1981; Vol. 1, Part 1a.

Horizoe, H.; Tanimoto, T.; Yamamoto, I.; Kano, Y. Phase Equilibrium Study for the Separation of Ethanol−Water-Solution Using Subcritical and Supercritical Hydrocarbon Solvent Extraction. *Fluid Phase Equilib.* **1993**, *84*, 297−320.

Huang, S.; Radosz, M. Equation of State for Small, Large, Polydisperse, and Associating Molecules: Extension to Fluid Mixtures. *Ind. Eng. Chem. Res.* **1991**, *30*, 1994−2005.

Jennings, D.; Lee, R. J.; Teja, A. Vapor-Liquid Equilibrium in the Carbon Dioxide + Ethanol and Carbon Dioxide + 1-Butanol Systems. *J. Chem. Eng. Data* **1991**, *36*, 303−307.

Leu, A.; Robinson, R. High-Pressure Vapor-Liquid Equilibrium Phase Properties of the Octafluoropropane (K-218)−Chlorodifluoromethane (R-22) Binary System. *J. Chem. Eng. Data* **1992**, *37*, 7−10.

McHugh, M.; Krukonis, V. *Supercritical Fluid Extraction*; Butterworth: Woburn, MA, 1986.

Nagahama, K.; Suzuki, J.; Suzuki, T. *High-Pressure Vapor−Liquid Equilibria for the Supercritical CO_2 + Ethanol + Water System*. Proceedings of the International Symposium on Supercritical Fluids, October 17−19, Nice, France; Societe Francaise de Chimie: Paris, 1988; Vol. 1, pp 143−150.

Ohgaki, K.; Katayama, T. Isothermal Vapor-Liquid Equilibrium Data for Binary Systems Containing Carbon Dioxide at High Pressures: Methanol-Carbon Dioxide, *n*-Hexane-Carbon Dioxide, and Benzene-Carbon Dioxide Systems. *J. Chem. Eng. Data* **1976**, *21*, 53−55.

Peng, Y.; Robinson, B. A New-Constant Equation of State. *Ind. Eng. Chem. Fundam.* **1976**, *15*, 59−64.

Radosz, M. Vapor-Liquid Equilibrium for 2-Propanol and Carbon Dioxide. *J. Chem. Eng. Data* **1986**, *31*, 43−45.

Suresh, S.; Elliott, J. Multiphase Equilibrium Analysis via a Generalized Equation of State for Associating Mixtures. *Ind. Eng. Chem. Res.* **1992**, *31*, 2783−2794.

Suzuki, K.; Sue, H. Isothermal Vapor-Liquid Equilibrium Data for Binary Systems at High Pressures: Carbon Dioxide-Methanol, Carbon Dioxide-Ethanol, Carbon Dioxide-1-propanol, Methane-Ethanol, Methane-1-Propanol, Ethane-Ethanol, and Ethane-1-Propanol Systems. *J. Chem. Eng. Data* **1990**, *35*, 63−66.

Tom, J.; Lim, G. B.; Debenedetti, P.; Prud'homme, R. *Application of Supercritical Fluids in the controlled Release of Drugs*; ACS

Symposium Series 514; American Chemical Society: Washington, DC, 1993; pp 238−257.

Tsang, C.; Streett, W. Vapor-Liquid Equilibrium in the System Carbon Dioxide /Dimethyl Ether. *J. Chem. Eng. Data* **1981**, *26*, 155−159.

Vargaftik, N. *Handbook of Physical Properties of Liquids and Gases*; Springer-Verlag: Berlin, 1975.

Xu, N.; Yao, J.; Wang, Y.; Shi, J.; Lu, B. Vapor-Liquid Equilibria of Five Binary Systems. *Fluid Phase Equilib.* **1991**, *69*, 261−270

Yoon, H.; Lee, H. S.; Lee, H. High-PressureVapor-Liquid Equilibria for the Carbon Dioxide + Methanol and Carbon Dioxide + Ethanol, and Carbon Dioxide + Methanol + Ethanol. *J. Chem. Eng. Data* **1993**, *38*, 53−55.

Received for review May 18, 1999. Accepted November 17, 1999. The authors gratefully acknowledge the partial support of this research by Chemstations, Inc., under Grant 6-38927, and British Petroleum under Grant 2-01210.

JE990136G